Prepared for submission to JCAP

Real-space computation of E/B-mode maps I: Formalism and Compact Kernels

Aditya Rotti and Kevin Huffenberger

Department of Physics, Florida State University, Keen Physics Building, 77 Chieftan Way, Tallahassee, Florida, U.S.A.

E-mail: adityarotti@gmail.com, khuffenberger@fsu.edu

Abstract. We derive full-sky, real-space operators that convert between polarization Stokes Q/U parameters to the coordinate-independent, scalar E/B modes that are widely used in Cosmic Microwave Background and cosmic shear analysis. The covolution kernels split naturally into angular and radial parts, and we show explicitly how the spatial extent of the convolution kernel depends on the targeted band-limit. We show that a arbitrary radial dependence can produce E/B-like maps and that these are simply filtered versions of the standard E/B maps. This allows us to compute E/B maps in real space with a compactly-supported kernel, an approach that can guarantee the avoidance of known foreground regions and can be employed in a massively parallel scheme at high-resolution. We can compute power spectra using standard techniques, and recover the power spectrum of the sky with a simple window function. We cast the standard CMB polarization analysis operators in a matrix-vector notation which facilitates the derivations and shows that the kernels relate directly to spin-0 $Y_{\ell 2}$ spherical harmonic functions. This new notation also allows us to derive real space operators which decompose the measured Stokes parameters into their even and odd-parity parts, without ever evaluating the scalar E/B fields themselves. This paper is the first part in a series of papers that explore real-space computation of polarization modes and their applications.

Contents

1 Introduction **1**

2 Polarization primer **2**
2.1 Matrix notation 3

3 Real space operators **5**
3.1 Evaluating scalar fields E & B from Stokes parameters Q & U 6
3.2 Evaluating Stokes parameters Q & U from scalar fields E & B 10
3.3 Decomposing Stokes parameters Q & U into those corresponding to E & B modes respectively 11
3.4 Visualizing the convolution kernels 13
3.5 Quantifying the non-locality of E & B modes 15

4 Generalized operators **16**
4.1 Recovering the default E and B mode spectra 20

5 Discussion **20**

6 Appendix **21**
6.1 Product of spin spherical harmonics 21

1 Introduction

The Cosmic Mircowave Background is 10 percent polarized, but the polarization contains independent cosmological information.

Standard technique is to convert Stokes parameters into scalar and pseudo-scalar modes, which are easier to compare to theory.

The pseudo-scalar B mode is particularly important because it cannot be generated by primordial scalar pertubations

primordial tensor perturbations

lensing of E-modes

systematics checks

exotic phenemena like cosmic birefringence

The spin-0 E/B modes relate to the spin-2 Stokes parameters via the spin-raising and -lowering operators $(\eth, \bar{\eth})$, which are second derivatives evaulated locally. However, in practice we compute E/B modes to a specified band limit, and this makes them non-local functions of the polarization field. In other words, the E/B modes at a point can get contributions from all over the sky.

(stuff about foregrounds, masking, ambiguous modes with references)

Zaldarriaga explored the spatial real-space kernels in the flat-sky approximation [].

In this work we follow the convection in which bar-ed variables correspond to those in real space, while the tilde-ed variables correspond to those in harmonic space [1].

This paper is organized in the following manner: In Sec. **??** we present a primer on the description of CMB polarization on the sphere and introduce the matrix notation which

provides a more concise description of the same. In Sec. 3 we introduce the necessary tools and discuss the derivations of the real space operators. In Sec. 3.4 we evaluate the real space operators and present visualizations of these functions. Here we also discuss the locality of the real space E & B operators. In Sec. **??** we implement these operators to evaluate E & B maps from the Stokes parameters Q & U and compare these maps and their spectra from those derived using Healpix. We conclude with a discussion and the scope of this new method of analyzing CMB polarization in Sec. 5.

2 Polarization primer

The CMB polarization is measured in terms of Stokes Q and U parameters. The Stokes Q is defined as the linear polarization measured along local cartesian axes (+ along the x-axis and − along the y-axis) while Stokes U is defined as the linear polarization measured along the cartesian axes rotated by 45° (+ along x-axis and − along the y-axis in the counter-clockwise rotated system). Clearly the definitions of Stokes parameters depend on the choice of the coordinate system and it can be shown that the measurement made in two different coordinate systems rotated by an angle ϕ are related by the following equation,

$$\begin{bmatrix} Q \\ U \end{bmatrix}' = \begin{bmatrix} \cos 2\psi & \sin 2\psi \\ -\sin 2\psi & \cos 2\psi \end{bmatrix} \begin{bmatrix} Q \\ U \end{bmatrix} , \tag{2.1}$$

which one can simply checked by verifying that $Q' \to U$ and $U' \to -Q$ when the coordinate systems are rotated by 45° in the counter-clockwise sense.

Following the notation of [2], fields which transform as,

$${}_sf' = e^{-is\psi}{}_sf , \tag{2.2}$$

under right handed rotations of the local coordinate system are termed spin-s fields. The Stokes parameters can be combined to define the complex fields,

$${}_{\pm2}\bar{X}(\hat{n}) = Q(\hat{n}) \pm iU(\hat{n}) , \tag{2.3}$$

which under rotation of the local tangent plane coordinate system by an angle ψ at any point on the sphere transform as: ${}_{\pm2}X' = e^{\mp i2\psi}{}_{\pm2}X$, which follows directly from Eq. (2.1). Therefore the quantities ${}_{\pm2}X$ are spin$\pm$2 fields respectively.

The Stokes parameters being coordinate dependent quantities it is inconvenient to work with them. It is possible to define spin raising ($\eth$) operator on the sphere which when operated on a field of spin-s ${}_sf$ results in a fields with spin-$(s+1)$: $(\eth_s f)' = e^{-i(s+1)\psi}(\eth_s f)$ and similarly one can define a spin lowering ($\bar{\eth}$) operators such that $(\bar{\eth}_s f)' = e^{-i(s-1)\psi}(\bar{\eth}_s f)$[3]. One can now construct a complex spin-0 scalar by applying the spin raising and lowering operators on the spin-2 fields ${}_{\pm2}X$ as follows,

$$\mathcal{E}(\hat{n}) + i\mathcal{B}(\hat{n}) = -\bar{\eth}^2_{+2}\bar{X}(\hat{n}) , \tag{2.4a}$$
$$\mathcal{E}(\hat{n}) - i\mathcal{B}(\hat{n}) = -\eth^2_{-2}\bar{X}(\hat{n}) , \tag{2.4b}$$

which by the virtue of being scalars are independent of coordinate definitions.

The complex field ${}_{\pm2}X$ defined on the sphere can be decomposed in spin spherical harmonic functions: ${}_{\pm2}X(\hat{n}) = \sum_{\ell m} {}_{\pm2}X_{\ell m}{}_{\pm2}Y_{\ell m}(\hat{n})$. On applying the spin raising and

lowering operators on the spin spherical harmonic functions leads to the following identities[3],

$$\eth_s Y_{lm}(\hat{n}) = \sqrt{(\ell - s)(\ell + s + 1)}_{s+1} Y_{lm}(\hat{n}) \,, \tag{2.5a}$$

$$\bar{\eth}_s Y_{lm}(\hat{n}) = -\sqrt{(\ell + s)(\ell - s + 1)}_{s-1} Y_{lm}(\hat{n}) \,, \tag{2.5b}$$

where ${}_sY_{lm}(\hat{n})$ denote the spin-s spherical harmonics.

Using Eq. (2.4), the spin spherical harmonic decomposition of ${}_{\pm2}X$ and the identities given in Eq. (2.5) it can be shown that the scalar fields $\mathcal{E}/\mathcal{B}$ are given by the following equations,

$$\mathcal{E}(\hat{n}) = \sum_{\ell m} a^E_{\ell m} \sqrt{\frac{(\ell+2)!}{(\ell-2)!}} Y_{\ell m}(\hat{n}) \;\; ; \;\; \mathcal{B}(\hat{n}) = \sum_{\ell m} a^B_{\ell m} \sqrt{\frac{(\ell+2)!}{(\ell-2)!}} Y_{\ell m}(\hat{n}) \,, \tag{2.6}$$

where the harmonic coefficients $a^E_{\ell m}$ & $a^B_{\ell m}$ are related to the harmonic coefficients of the spin-2 polarization field via the following equations,

$$a^E_{\ell m} = -\frac{1}{2}\left[{}_{+2}\tilde{X}_{\ell m} + {}_{-2}\tilde{X}_{\ell m}\right] \;\; ; \;\; a^B_{\ell m} = -\frac{1}{2i}\left[{}_{+2}\tilde{X}_{\ell m} - {}_{-2}\tilde{X}_{\ell m}\right] . \tag{2.7}$$

In the remainder of this article, we will work with the scalar E and pseudo scalar B fields as defined by the following equations,

$$E(\hat{n}) = \sum_{\ell m} a^E_{\ell m} Y_{\ell m}(\hat{n}) \;\; ; \;\; B(\hat{n}) = \sum_{\ell m} a^B_{\ell m} Y_{\ell m}(\hat{n}) \,. \tag{2.8}$$

Note that these E/B fields are merely filtered versions of $\mathcal{E}/\mathcal{B}$ as their spherical harmonic coefficients of expansion are related by the factor $\sqrt{\frac{(\ell+2)!}{(\ell-2)!}}$.

2.1 Matrix notation

In this section we cast the relations introduced in Sec. 2 in matrix notation[1]. This representation will make transparent the derivation of the real space operators we discuss in the following sections. We adopt a convention in which real space quantities are denoted by bar-ed variable while those in harmonic space are denoted by tilde-ed variables.

We begin by introducing the matrices encoding the spin spherical harmonic basis vectors,

$${}_{|s|}\mathcal{Y} = \begin{bmatrix} {}_{+s}Y & 0 \\ 0 & {}_{-s}Y \end{bmatrix}_{2\mathrm{N_{pix}} \times 2\mathrm{N_{alms}}} , \tag{2.9}$$

where s denotes the spin of the basis functions. For this work we will be working with cases $s \in [0, 2]$. In this notation, each column can be mapped to a specific harmonic basis function marked by the pair of indices: (ℓ, m) and each row maps to a specific position on the sphere. Note that this matrix is in general not a square matrix. The number of rows is determined by the scheme used to discretely represent the sphere and the number of columns is set by the number of basis functions of interest (often determined by the band limit).

[1] While we work with the matrix and vector sizes given in terms of some pixelization parameter $\mathrm{N_{pix}}$, all the relations are equally valid in the continuum limit attained by allowing $\mathrm{N_{pix}} \to \infty$

We now define the different polarization data vectors and their representation in real and harmonic space as follows,

$$\bar{S} = \begin{bmatrix} E \\ B \end{bmatrix}_{2\mathrm{N_{pix}}\times 1} \quad ; \quad \bar{X} = \begin{bmatrix} {}_{+2}X \\ {}_{-2}X \end{bmatrix}_{2\mathrm{N_{pix}}\times 1} \quad ; \quad \bar{P} = \begin{bmatrix} Q \\ U \end{bmatrix}_{2\mathrm{N_{pix}}\times 1} , \tag{2.10a}$$

$$\tilde{S} = \begin{bmatrix} a^E \\ a^B \end{bmatrix}_{2\mathrm{N_{alms}}\times 1} \quad ; \quad \tilde{X} = \begin{bmatrix} {}_{+2}\tilde{X} \\ {}_{-2}\tilde{X} \end{bmatrix}_{2\mathrm{N_{alms}}\times 1} . \tag{2.10b}$$

The different symbols have the same meaning as that discussed in Sec. 2, except that the subscript $_{\ell m}$ for the spherical harmonic coefficients of expansion is suppressed in favor of cleaner notation.

Next we define the operators which govern the transformations between different representations of the polarization field as follows,

$$\bar{T} = \begin{bmatrix} \mathbb{1} & i\mathbb{1} \\ \mathbb{1} & -i\mathbb{1} \end{bmatrix}_{2\mathrm{N_{pix}}\times 2\mathrm{N_{pix}}} \quad ; \quad \bar{T}^{-1} = \frac{1}{2}\bar{T}^{\dagger} , \tag{2.11a}$$

$$\tilde{T} = -\begin{bmatrix} \mathbb{1} & i\mathbb{1} \\ \mathbb{1} & -i\mathbb{1} \end{bmatrix}_{2\mathrm{N_{alms}}\times 2\mathrm{N_{alms}}} \quad ; \quad \tilde{T}^{-1} = \frac{1}{2}\tilde{T}^{\dagger} , \tag{2.11b}$$

where we have chosen the sign conventions so as to match those used in Healpix. Using the data vectors and the matrix operators defined above we can now express, in compact notation, the forward and inverse relations between different representations of the polarization data vectors as follows,

$$\bar{X} = \bar{T} * \bar{P} \quad ; \quad \bar{P} = \frac{1}{2}\bar{T}^{\dagger} * \bar{X} , \tag{2.12a}$$

$$\bar{X} = {}_2\mathcal{Y} * \tilde{X} \quad ; \quad \tilde{X} = {}_2\mathcal{Y}^{\dagger} * \bar{X} , \tag{2.12b}$$

$$\tilde{X} = \tilde{T} * \tilde{S} \quad ; \quad \tilde{S} = \frac{1}{2}\tilde{T}^{\dagger} * \tilde{X} . \tag{2.12c}$$

$$\bar{S} = {}_0\mathcal{Y} * \tilde{S} \quad ; \quad \tilde{S} = {}_0\mathcal{Y}^{\dagger} * \bar{S} . \tag{2.12d}$$

Finally we introduce the harmonic space operators, which project the harmonic space data vector to E or B subspace,

$$\tilde{O}_E = \begin{bmatrix} \mathbb{1} & \mathbb{0} \\ \mathbb{0} & \mathbb{0} \end{bmatrix}_{2\mathrm{N_{alms}}\times 2\mathrm{N_{alms}}} \quad ; \quad \tilde{S}_E = \tilde{O}_E * \tilde{S} , \tag{2.13a}$$

$$\tilde{O}_B = \begin{bmatrix} \mathbb{0} & \mathbb{0} \\ \mathbb{0} & \mathbb{1} \end{bmatrix}_{2\mathrm{N_{alms}}\times 2\mathrm{N_{alms}}} \quad ; \quad \tilde{S}_B = \tilde{O}_B * \tilde{S} \tag{2.13b}$$

Note that these harmonic space matrices are idempotent, orthogonal to each other and their sum is an identity matrix as can be explicitly seen via the following relations,

$$\tilde{O}_E * \tilde{O}_E = \tilde{O}_E \quad ; \quad \tilde{O}_B * \tilde{O}_B = \tilde{O}_B , \tag{2.14a}$$

$$\tilde{O}_E * \tilde{O}_B = \mathbb{0} , \tag{2.14b}$$

$$\tilde{O}_E + \tilde{O}_B = \mathbb{1} . \tag{2.14c}$$

Note that the above relations for these harmonic space operators are exactly valid. In the following sections we aim to derive the real space analogues of these harmonic space operators.

3 Real space operators

The vector-matrix notation introduced in Sec. 2.1 allows for concise book keeping of all the operations involved in the analysis of CMB polarization. In this section we use this notation to derive the real space operators which translate the Stokes vector $\bar{P}$ to the vector of scalars $\bar{S}$ and vice versa. This vector-matrix notation also allows us to simply derive real space operators for direct decomposition of the Stokes vector $\bar{P}$ in to a vector $\bar{P}_E$ that correspond to E-modes and another vector $\bar{P}_B$ that corresponds to the B-modes of polarization, such that $\bar{P} = \bar{P}_E + \bar{P}_B$, without ever evaluating the E & B fields or their spherical harmonics. All the real space operators we derive are most conveniently expressed as functions of the Euler angles α, β & γ on the sphere. Owing to this, we begin with a brief discussion on Euler angles and present a visual method to think about them.

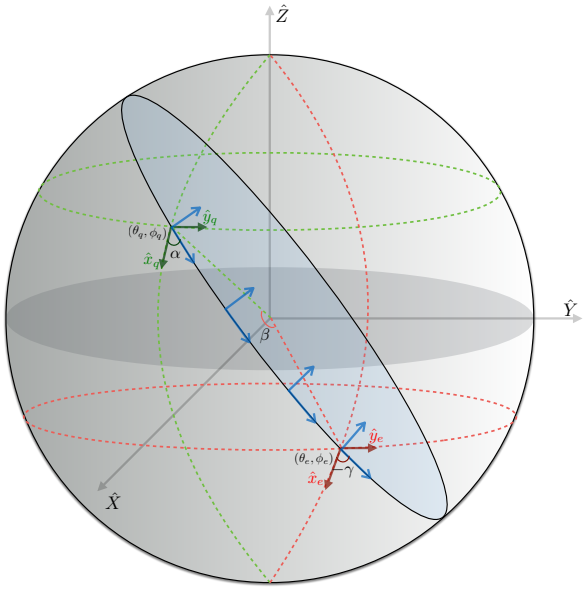

Figure 1. This figure depicts the Euler angles in the z-y1-z2 convention. The cartesian coordinates shown in dark green are those that lie in the tangent plane at location $\hat{n}_q = (\theta_q, \phi_q)$ while those shown in dark red are the ones that lie in the tangent plane at location $\hat{n}_e = (\theta_e, \phi_e)$. The blue coordinates at different locations are representative of the parallel transport along the geodesic connection the two locations $\hat{n}_q$ & $\hat{n}_e$ on the sphere.

Euler angles: We define the local cartesian coordinate system at any point on the sphere such that the z-axis points along the radial direction, the x-axis is along the vector tangent to the local longitude pointing south and the y-axis is a vector tangent to the local latitude pointing east as shown in Fig. 1. The Euler angles α, β & γ define rotation operations that transforms the local cartesian coordinate system defined at the location $\hat{n}_q \equiv (\theta_q, \phi_q)$ such that it aligns with the local cartesian coordinate system at the location $\hat{n}_e \equiv (\theta_e, \phi_e)$ [4].

For this work, it is convenient to think in the z-y1-z2 convention therefore all future references to Euler angles are in this convention[2]. In the z-y1-z2 convention, α defines the rotation about the z-axis, β defines the rotation about the new y-axis (y1-axis) after the previous rotation and γ defines the rotation about the final z-axis (z2-axis) after carrying out

[2]The Euler angles in the more standard $z-y-z$ convention are related to those in the $z-y1-z2$ convection by the following rule: $(\alpha, \beta, \gamma)_{z-y-z} = (\gamma, \beta, \alpha)_{z-y1-z2}$ [4].

the previous two rotations. These angles can be understood as follows: The rotation by α about the original z-axis is such that it aligns the x-axis of the cartesian system at location $\hat{n}_q$ along the great circle in the direction of shortest arc length towards $\hat{n}_e$. The rotation by β about the y2-axis parallel transports the local cartesian coordinate system from location $\hat{n}_q$ to location $\hat{n}_e$, such that the z-axes of the two coordinate systems are parallel to each other. Finally the rotation by angle γ about the z2-axis aligns the x & y axes of the parallel transported system with those of the local cartesian system defined at $\hat{n}_e$. The different Euler angles and the corresponding rotations are schematically represented in Fig. 1.

The simplest scenario is when one of the coordinates coincides with the north pole $\hat{n}_q = (\theta_q, \phi_q) = (0, 0)$ (the local cartesian system at this point being defined with an arbitrary convention set by choosing $\theta_0 \to 0$ while moving along the longitude $\phi_0 = 0$), in which case it is easy to see that rotations by Euler angles: $(\alpha, \beta, \gamma) = (\phi_e, \theta_e, 0)$ will align the cartesian system at $\hat{n}_q$ with that defined at position $\hat{n}_e$.

3.1 Evaluating scalar fields E & B from Stokes parameters Q & U

In Sec. 2 we described the standard procedure of computing the scalar fields E & B from the Stokes parameters Q & U. Here we derive the real space convolution kernels on the sphere, which can be used to directly evaluate the scalar fields E & B on the sphere. We use the relations given in Eq. (2.12), to write down an equation relating the real space vector of scalars $\bar{S}$ to the Stokes polarization vector $\bar{P}$,

$$\bar{S} = {}_0\mathcal{Y} * \tilde{T}^{-1} * {}_2\mathcal{Y}^\dagger * \bar{T} * \bar{P} = \frac{1}{2}{}_0\mathcal{Y} * \tilde{T}^\dagger * {}_2\mathcal{Y}^\dagger * \bar{T} * \bar{P}\,, \tag{3.1a}$$

$$= \bar{O} * \bar{P}\,. \tag{3.1b}$$

The explicit form of the real space operator $\bar{O}$ can be derived by contracting over all the matrix operators. This procedure of contracting over the operators is explicitly worked out in the following set of equations,

$$\bar{O} = \frac{1}{2}{}_0\mathcal{Y} * \tilde{T}^\dagger * {}_2\mathcal{Y}^\dagger * \bar{T}\,, \tag{3.2a}$$

$$= -0.5 \begin{bmatrix} {}_0Y_e & 0 \\ 0 & {}_0Y_e \end{bmatrix} \begin{bmatrix} \mathbb{1} & \mathbb{1} \\ -i\mathbb{1} & i\mathbb{1} \end{bmatrix} \begin{bmatrix} {}_{+2}Y_q^{T*} & 0 \\ 0 & {}_{-2}Y_q^{T*} \end{bmatrix} \begin{bmatrix} \mathbb{1} & i\mathbb{1} \\ \mathbb{1} & -i\mathbb{1} \end{bmatrix}, \tag{3.2b}$$

$$= -0.5 \begin{bmatrix} \sum({}_0Y_e\ {}_2Y_q^{T*} + {}_0Y_e\ {}_{-2}Y_q^{T*}) & \mathrm{i}\sum({}_0Y_e\ {}_2Y_q^{T*} - {}_0Y_e\ {}_{-2}Y_q^{T*}) \\ -\mathrm{i}\sum({}_0Y_e\ {}_2Y_q^{T*} - {}_0Y_e\ {}_{-2}Y_q^{T*}) & \sum({}_0Y_e\ {}_2Y_q^{T*} + {}_0Y_e\ {}_{-2}Y_q^{T*}) \end{bmatrix}, \tag{3.2c}$$

where the symbol ${}_0Y_e$ is used to denote the sub-matrix ${}_0Y_{\hat{n}_e \times \ell m} \equiv {}_0Y_{\ell m}(\hat{n}_e)$, the symbol ${}_{\pm 2}Y_q^{T*}$ is used to denote the matrix ${}_{\pm 2}Y^*_{\ell m \times \hat{n}_q} \equiv {}_{\pm 2}Y^*_{\ell m}(\hat{n}_q)$ and the summation is over the multipole indices ℓ, m. We purposefully use the index "e" to denote the location where the scalar fields are being evaluated and the index "q" to denote the location from which the Stokes parameters are being accessed. Using the conjugation properties of the spin spherical harmonic functions it can be shown that the following relation holds true, $\Rightarrow$ These constructions are dyadics

$$\left[\sum_{\ell m} {}_0Y_{\ell m}(\hat{n}_e)\,{}_{+2}Y^*_{\ell m}(\hat{n}_q)\right]^* = \sum_{\ell m} {}_0Y_{\ell m}(\hat{n}_e)\,{}_{-2}Y^*_{\ell m}(\hat{n}_q)\,. \tag{3.3}$$

where the terms on either side of the equation are those that appear in Eq. (3.2c). Note that each sub-matrix in Eq. (3.2c) is formed by some linear combination of a complex number

and its conjugate and is hence real. The m sum over the product of two spherical harmonic functions with spins s_1 and s_2 respectively, is given by the following identity [4],

$$\sum_m {}_{s_1}Y^*_{\ell m}(\hat{n}_i)\,{}_{s_2}Y_{\ell m}(\hat{n}_j) = \sqrt{\frac{2\ell+1}{4\pi}}\,{}_{s_2}Y_{\ell\,-s_1}(\beta_{ij},\alpha_{ij})e^{-is_2\gamma_{ij}}\,, \tag{3.4}$$

where α_{ij}, β_{ij} & γ_{ij} denote the Euler angles. Therefore the different parts of the real space operator $\bar{O}$ are completely specified in terms of the complex function,

$$\begin{aligned}
\mathcal{M}(\hat{n}_e,\hat{n}_q) &= \mathcal{M}_r + i\mathcal{M}_i\,,\\
&= \sum_{\ell m} {}_0Y_{\ell m}(\hat{n}_e)\,{}_{-2}Y^*_{\ell m}(\hat{n}_q) = \sum_{\ell}\sqrt{\frac{2\ell+1}{4\pi}}\,{}_0Y_{\ell 2}(\beta_{qe},\alpha_{qe})\,, &\text{(3.5a)}\\
&= \Big[\cos(2\alpha_{qe}) + i\sin(2\alpha_{qe})\Big]\sum_{\ell=\ell_{\rm min}}^{\ell_{\rm max}}\frac{2\ell+1}{4\pi}\sqrt{\frac{(\ell-2)!}{(\ell+2)!}}P_{\ell 2}(\cos\beta_{qe})\,, &\text{(3.5b)}\\
&= \Big[\cos(2\alpha_{qe}) + i\sin(2\alpha_{qe})\Big]\mathcal{M}f(\beta_{qe},\ell_{\rm min},\ell_{\rm max})\,, &\text{(3.5c)}
\end{aligned}$$

where we have used the identity given in Eq. (3.4) to simplify the product of the spherical harmonic functions. On simplifying Eq. (3.2c), the local convolution kernel can be cast in this simple form,

$$\bar{O} = -\begin{bmatrix}\mathcal{M}_r & \mathcal{M}_i\\ -\mathcal{M}_i & \mathcal{M}_r\end{bmatrix}_{2N_{\rm pix}\times 2N_{pix}} = -\mathcal{M}f(\beta_{qe},\ell_{\rm min},\ell_{\rm max})\begin{bmatrix}\cos(2\alpha_{qe}) & \sin(2\alpha_{qe})\\ -\sin(2\alpha_{qe}) & \cos(2\alpha_{qe})\end{bmatrix}\,. \tag{3.6}$$

Specifically note that α_{qe}, β_{qe} & γ_{qe} denote the Euler angles which rotate the local cartesian system at the location $\hat{n}_q$ where the Stokes field is measured to the cartesian system at the location $\hat{n}_e$ where the scalar fields are evaluated: $\hat{n}_q \xrightarrow{\mathcal{R}(\alpha_{qe},\beta_{qe},\gamma_{qe})} \hat{n}_e$. The Euler angles for the inverse rotations are given by the Euler angles $\alpha_{eq} = -\gamma_{qe}$, $\beta_{eq} = -\beta_{qe}$ and $\gamma_{eq} = -\alpha_{qe}$[4]. Since the kernel only depends on the cosine of the Euler angle β, it is immune to changes in its sign. More importantly, the ordering of indices on the Euler angle α and γ is important and leads to two different interpretations of the real space kernels.

Convolution: Working from the frame of the pixel "e" where the scalar modes need to be evaluated, the Euler angles to the surrounding pixels are: $\alpha_{eq},\beta_{eq},\gamma_{eq}$. In terms of these Euler angles, the value of scalar fields E & B at the central pixel "e" can be evaluated by convolving over the measured Stokes Q & U parameters in the surrounding pixels marked by indices "q". Specifically, the convolution is fully defined in terms of the Euler angles β_{eq} & γ_{eq} and is given by the following equation,

$$\begin{bmatrix}E_e\\ B_e\end{bmatrix} = -\sum_{q=1}^{N_{\rm pix}}\mathcal{M}f(\beta_{eq},\ell_{\rm min},\ell_{\rm max})\begin{bmatrix}\cos(2\gamma_{eq}) & -\sin(2\gamma_{eq})\\ \sin(2\gamma_{eq}) & \cos(2\gamma_{eq})\end{bmatrix}\begin{bmatrix}Q_q\\ U_q\end{bmatrix}\Delta\Omega\,, \tag{3.7}$$

where $\Delta\Omega$ denotes the pixel area and all the symbols have their usual meaning. When written in terms of the complex spin-0 field $[E+iB]$ and the spin-2 field ${}_{+2}X$, the above equation

can be expressed more concisely as follows,

$$[E+iB](\hat{n}_e) = -\Delta\Omega \sum_{q=1}^{N_{\rm pix}} \left(\sum_{\ell=\ell_{\rm min}}^{\ell_{\rm max}} \frac{2\ell+1}{4\pi} \sqrt{\frac{(\ell-2)!}{(\ell+2)!}} P_\ell^2(\beta_{eq}) \right) \left(e^{i2\gamma_{eq}} {}_{+2}X(\hat{n}_q) \right), \quad (3.8a)$$

$$= \left\{ \left[-\Delta\Omega \sum_{\ell=\ell_{\rm min}}^{\ell_{\rm max}} \sqrt{\frac{2\ell+1}{4\pi}} Y_{\ell 2}(\beta_{eq}, \gamma_{eq}) \right] \circ {}_{+2}X \right\}(\hat{n}_e), \quad (3.8b)$$

$$= \left\{ \mathcal{M}_{Beam} \circ {}_{+2}X \right\}(\hat{n}_e), \quad (3.8c)$$

where $\circ$ denotes the convolution and the spherical harmonic functions denote the rotated functions such that the pole of the function coincides with the direction $\hat{n}_e$. *Radiating:*

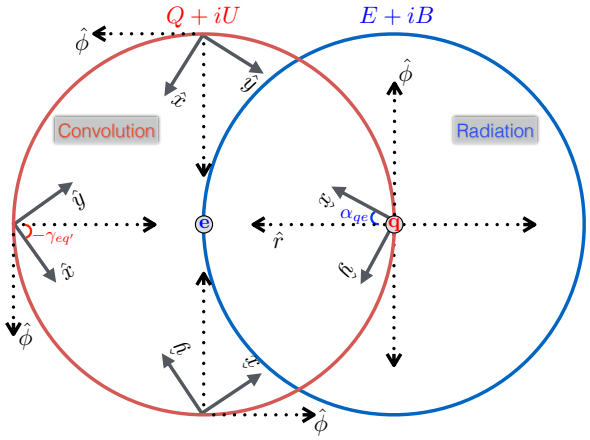

Figure 2. The local cartesian coordinate are only drawn on the red circle, representative of the coordinate dependence of the Stokes parameters. The coordinates are not drawn on the blue circle representing the fact that the value of the scalar field does not depend of the coordinate definition. The value of the scalar field at the specific location 'e' can be evaluated by summing over the contribution from all the Stokes parameters on the red circle (sphere). The convolutions are performed with kernels which are defined in term of the Euler angle γ_{eq}. Alternatively, if centered on 'q' then one can compute the contribution from the Stokes parameter at this specific location to all the point on the blue circle(sphere). The contribution across the sky from the Stokes parameter at the location 'q' is given by a function of the Euler angle α_{eq}. In the flat sky limit, since $\gamma = -\alpha$ there is no difference between the radiating and convolving kernels.

On the contrary, while working from the frame of the pixel "q", the Euler angles to the surrounding pixels are: $\alpha_{qe}, \beta_{qe}, \gamma_{qe}$. The E & B mode maps resulting from the Stokes Q & U parameters specified at the location $\hat{n}_q$ is given by the following expression,

$$\bar{S}_q = \begin{bmatrix} E_e \\ B_e \end{bmatrix}_q = -\mathcal{M} f(\beta_{qe}, \ell_{\rm min}, \ell_{\rm max}) \begin{bmatrix} \cos(2\alpha_{qe}) & \sin(2\alpha_{qe}) \\ -\sin(2\alpha_{qe}) & \cos(2\alpha_{qe}) \end{bmatrix} \begin{bmatrix} Q_q \\ U_q \end{bmatrix} \Delta\Omega\,. \quad (3.9)$$

The total map of E & B modes can be simply evaluated by summing over the contribution from the Stokes parameters at each location $\hat{n}_q$: $\bar{S} = \sum_{q=1}^{N_{\rm pix}} \bar{S}_q$. The above expression can

again be cast in a more concise form as follows,

$$[E+iB] = -\Delta\Omega \sum_{q=1}^{N_{\rm pix}} \Big[{}_{+2}X(\hat{n}_q) e^{-i2\alpha_{qe}} \Big] {}_{\mathcal{M}}f(\beta_{qe}) \,, \tag{3.10a}$$

$$= \sum_{q=1}^{N_{\rm pix}} \left\{ {}_{+2}X(\hat{n}_q) \cdot \left[-\Delta\Omega \sum_{\ell=\ell_{\rm min}}^{\ell_{\rm max}} \sqrt{\frac{2\ell+1}{4\pi}} Y^*_{\ell 2}(\beta_{qe}, \alpha_{qe}) \right] \right\} , \tag{3.10b}$$

$$= \sum_{q=1}^{N_{\rm pix}} {}_{+2}X(\hat{n}_q) \cdot \mathcal{M}_{Green}(\hat{n}_q) \,, \tag{3.10c}$$

where "$\cdot$" denotes a simple scalar multiplication. $\mathcal{M}_{Green}(\hat{n}_q)$ is response of the real space operator $\bar{O}$ when operated on a Stokes field: $\delta(\hat{n}-\hat{n}_q) + i\delta(\hat{n}-\hat{n}_q)$, hence it can be thought of as the Green's function of the real space operator. $\Rightarrow$ Is this interpretation correct ? Is the complex delta function a spin 2 function ?

Recall that the product of two functions with spins s_1 and s_2 results in a function with spin $s_1 + s_2$: ${}_{s_1+s_2}f = {}_{s_1}g\,{}_{s_2}h$ $\Rightarrow$ The following argument is that of the product of a number with a field, so is this relevant ?. If one rotates the cartesian coordinates in the tangent plane at location $\hat{n}_q$ by an angle ϕ about the local $\hat{z}_q$ axis, the Stokes parameters in the new rotated frame are given by: ${}_{+2}X(\hat{n}_q) \xrightarrow{\mathcal{R}_{\hat{z}_q}(\phi)} {}_{+2}X(\hat{n}_q)e^{-i2\phi}$. Recall that the Euler angle α_{qe} in the $z-y_1-z_2$ sense of rotations is such that it aligns the local $\hat{x}_q$-axis along the geodesic in the direction of $\hat{n}_e$. Now if the local planar axes are already rotated by an angle ϕ then $\alpha_{qe} \to \alpha_{qe} - \phi$ and therefore one can see that: $e^{-i2\alpha_{qe}} \xrightarrow{\mathcal{R}_{\hat{z}_q}(\phi)} e^{-i2\alpha_{qe}} e^{i2\phi}$. The Euler angles $|\beta_{qe}|$ which measure the angular distance between pixels remains unaltered under this local rotation operation. Given these transformation properties one can now note that the product ${}_{+2}X(\hat{n}_q)e^{-i2\alpha_{qe}}$ is invariant under rotations $\mathcal{R}_{\hat{z}_q}(\phi)$ and hence must form a spin-0 field. This argument makes intuitive, the construction of the spin-0 E and B modes of polarization from the measured Stokes parameters. Here it is also interesting to note that the E-modes are constructed by product of functions $(U\sin 2\alpha, Q\cos 2\alpha)$ which have the same parity and hence have even parity while the B-modes are constructed by multiplying functions $(Q\sin 2\alpha, U\cos 2\alpha)$ of opposite parity and hence have an odd parity.

Using Eq. (3.9) one can see that when $q = e$ ($\beta_{qq} = 0$, $\alpha_{qq} = 0, 2\pi, 4\pi, ...$): $E_q = -{}_{\mathcal{M}}f(\beta_{qq})Q_q$ and $B_q = -{}_{\mathcal{M}}f(\beta_{qq})U_q$ which does not transform as a spin-0 field under local rotations unless ${}_{\mathcal{M}}f(\beta_{qq}=0) = 0$. One can make a similar argument when pixels "q" and "e" are diametrically opposite. Therefore the radial kernels have to satisfy the constraint that they vanish at $\beta = 0, \pi$. The radial kernel ${}_{\mathcal{M}}f(\beta)$ is constructed by forming a weighted linear combination of P^2_ℓ Legendre polynomials which have the following limiting form: $P^2_\ell(\beta) \propto \sin^2\beta \to 0$ as $\beta \to 0, \pi$ and therefore satisfy this necessary constraint.

The real space operator has a azimuthal part which depends only on the Euler angle $\alpha_{qe}(\gamma_{eq})$, has no multipole ℓ dependence and is the crucial operation which translates between the two different spin representation of CMB polarization. The radial part of the kernel is specified by the function ${}_{\mathcal{M}}f(\beta, \ell_{\rm min}, \ell_{\rm max})$, it depends only on the angular separation $|\beta_{eq}|$ between pixels and completely incorporates the multipole ℓ dependence of the kernel. It's the radial part of the kernel that determines the locality of the real space operator.

3.2 Evaluating Stokes parameters Q & U from scalar fields E & B

The real space operator which translates E & B fields to Stokes parameters Q & U can be derived using a similar procedure. The inverse operator is given by the following expression,

$$\bar{P} = \bar{T}^{-1} *_2\mathcal{Y} * \tilde{T} *_0\mathcal{Y}^\dagger \bar{S} = \frac{1}{2}\bar{T}^\dagger *_2\mathcal{Y} * \tilde{T} *_0\mathcal{Y}^\dagger \bar{S}\,, \tag{3.11a}$$

$$= \bar{O}^{-1} * \bar{S}\,. \tag{3.11b}$$

Providing the explicit derivation here will be redundant with that described in the previous sections and hence we avoid that. The inverse operator $\bar{O}^{-1}$ can be derived by realizing that $\mathcal{M}^{-1}$ is given by the following expression,

$$\mathcal{M}^{-1} = \sum_{\ell m} {}_2Y_{\ell m}(\hat{n}_q)\,{}_0Y^*_{\ell m}(\hat{n}_e) \tag{3.12}$$

The inverse operator is given by the following expression,

$$\bar{O}^{-1} = -\begin{bmatrix}\mathcal{M}_r & -\mathcal{M}_i \\ \mathcal{M}_i & \mathcal{M}_r\end{bmatrix}_{2N_{\rm pix}\times 2N_{pix}} = -{}_{\mathcal{M}}f(\beta_{eq},\ell_{\rm min},\ell_{\rm max})\begin{bmatrix}\cos(2\alpha_{eq}) & -\sin(2\alpha_{eq}) \\ \sin(2\alpha_{eq}) & \cos(2\alpha_{eq})\end{bmatrix}. \tag{3.13}$$

where all the symbols have the same meaning as discussed in Sec. 3.1. Note that the kernel in the above equation differs from the one in Eq. (3.6) by a change in sign on the off-diagonals of the block matrix and the pixel indexing is reversed $e \leftrightarrow q$. We can evaluate the Stokes parameters Q & U from the scalar fields E & B by evaluating the following expression,

$$\begin{bmatrix}Q_i \\ U_i\end{bmatrix} = -\Delta\Omega\sum_{j=1}^{N_{\rm pix}} {}_{\mathcal{M}}f(\beta_{ij},\ell_{\rm min},\ell_{\rm max})\begin{bmatrix}\cos(2\alpha_{ij}) & -\sin(2\alpha_{ij}) \\ \sin(2\alpha_{ij}) & \cos(2\alpha_{ij})\end{bmatrix}\begin{bmatrix}E_j \\ B_j\end{bmatrix}, \tag{3.14}$$

where all the symbols have their usual meaning. The above equation can again be expressed more concisely as follows,

$${}_{+2}\bar{X}(\hat{n}_0) = -\Delta\Omega\sum_{j=1}^{N_{\rm pix}}\left(\sum_{\ell=\ell_{\rm min}}^{\ell_{\rm max}}\frac{2\ell+1}{4\pi}\sqrt{\frac{(\ell-2)!}{(\ell+2)!}}P^2_\ell(\beta_{0j})\right)\left(e^{i2\alpha_{0j}}[E+iB](\hat{n}_j)\right), \tag{3.15a}$$

$$= -\left\{\left[\sum_{\ell=\ell_{\rm min}}^{\ell_{\rm max}}\sqrt{\frac{2\ell+1}{4\pi}}Y_{\ell 2}\right]\circ[E+iB]\right\}(\hat{n}_0)\,, \tag{3.15b}$$

$$= -\Big\{\mathcal{M}\circ[E+iB]\Big\}(\hat{n}_0)\,, \tag{3.15c}$$

which $\circ$ is to be interpreted as a convolution. The only change in the convolution kernel as compared to that in Eq. (**??**) is that the $Y_{\ell 2}$ functions are not conjugated. This can again be simply understood as the construction of a spin-2 field by taking a product of a spin-0 field $[E+iB]$ with a spin $+2$ field $e^{+i2\alpha}$. The radial dependence of the operator $\bar{O}^{-1}$ is identical to the that of $\bar{O}$ as one may have expected. From the perspective of the scalar field $[E+iB]$, all the coordinate dependence of the Stokes parameters is encoded in the function $e^{+i2\alpha}$. The radial functions again have to vanish at $\beta \to 0, \pi$ for the same reasons that the function $e^{+i2\alpha}$ is ill defined at these locations.

3.3 Decomposing Stokes parameters Q & U into those corresponding to E & B modes respectively

We can only measure the total Stokes vector which is a sum of the Stokes vectors corresponding to the respective scalar modes. The E & B modes are orthogonal to each other, in the sense that their respective operators are orthogonal to each other as seen in Eq. (2.14b). It is possible to decompose the Stokes vector $\bar{P}$ into one $\bar{P}_{\rm E}$ that purely contributes to E modes and another $\bar{P}_{\rm B}$ that purely contribute to the B modes of polarization. In this section we derive the real space operators which operate on the total Stokes vector and yield this decomposition, without ever having to explicitly evaluate the scalar modes. Though the algebra is a little more involved, the derivation is similar to that discussed in Sec. 3.1, hence we refrain from presenting the detailed calculations here, but outline the key points. We use the harmonic space projection operators $\tilde{O}_{E/B}$, defined in Eq. (2.13), to derive the respective real space operators. The Stokes parameters corresponding to each scalar mode are given by the following expressions,

$$\begin{aligned}
\bar{P}_E &= [\bar{T}^{-1} * {}_2\mathcal{Y} * \tilde{T} * \tilde{O}_E * \tilde{T}^{-1} * {}_2\mathcal{Y}^\dagger * \bar{T}] * \bar{P}\,, \qquad (3.16)\\
&= [\frac{1}{4}\bar{T}^\dagger * {}_2\mathcal{Y} * \tilde{T} * \tilde{O}_E * \tilde{T}^\dagger * {}_2\mathcal{Y}^\dagger * \bar{T}] * \bar{P}\,,\\
&= \bar{O}_E * \bar{P}\,,\\
\bar{P}_B &= [\bar{T}^{-1} * {}_2\mathcal{Y} * \tilde{T} * \tilde{O}_B * \tilde{T}^{-1} * {}_2\mathcal{Y}^\dagger * \bar{T}] * \bar{P}\,, \qquad (3.17)\\
&= [\frac{1}{4}\bar{T}^\dagger * {}_2\mathcal{Y} * \tilde{T} * \tilde{O}_B * \tilde{T}^\dagger * {}_2\mathcal{Y}^\dagger * \bar{T}] * \bar{P}\,,\\
&= \bar{O}_B * \bar{P}\,.
\end{aligned}$$

We contract over all the matrix operators to arrive at the the real space operators. On working through the algebra it can be shown that the real space operators have the following form,

$$\bar{O}_{E/B} = 0.5 \begin{bmatrix} \mathcal{I}_r & \mathcal{I}_i \\ -\mathcal{I}_i & \mathcal{I}_r \end{bmatrix} \pm \begin{bmatrix} \mathcal{D}_r & \mathcal{D}_i \\ \mathcal{D}_i & -\mathcal{D}_r \end{bmatrix}\,, \qquad (3.18)$$

where $\mathcal{I}_r$ & $\mathcal{D}_r$ and $\mathcal{I}_i$ & $\mathcal{D}_i$ are the real and complex parts of the following complex functions,

$$\mathcal{I} = \mathcal{I}_r + i\mathcal{I}_i = \sum_{\ell m} {}_{-2}Y_{\ell m}(\hat{n}_i)\,{}_{-2}Y^*_{\ell m}(\hat{n}_j)\,, \qquad (3.19a)$$

$$\mathcal{D} = \mathcal{D}_r + i\mathcal{D}_i = \sum_{\ell m} {}_{2}Y_{\ell m}(\hat{n}_i)\,{}_{-2}Y^*_{\ell m}(\hat{n}_j)\,. \qquad (3.19b)$$

These functions can be further simplified using the identity of spin spherical harmonics given in Eq. (3.4). Specifically it can be shown that these functions reduce to the following mathematical forms,

$$\mathcal{I}(\hat{n}_i, \hat{n}_j) = \sum_\ell \sqrt{\frac{2\ell+1}{4\pi}}\,{}_{-2}Y_{\ell 2}(\beta_{ij}, \alpha_{ij})\ \mathrm{e}^{\mathrm{i}2\gamma_{\rm ij}} = \mathcal{I}_{\rm r} + \mathrm{i}\mathcal{I}_{\rm i}\,, \qquad (3.20a)$$

$$\mathcal{I}_r + i\mathcal{I}_i = \Big[\cos(2\alpha_{ij} + 2\gamma_{ij}) + i\sin(2\alpha_{ij} + 2\gamma_{ij})\Big]_{\mathcal{I}} f(\beta_{ij}, \ell_{\rm min}, \ell_{\rm max})\,, \qquad (3.20b)$$

$$\mathcal{D}(\hat{n}_i, \hat{n}_j) = \sum_{\ell} \sqrt{\frac{2\ell+1}{4\pi}} {}_2Y_{\ell 2}(\beta_{ij}, \alpha_{ij})\ \mathrm{e}^{-\mathrm{i}2\gamma_{\mathrm{ij}}} = \mathcal{D}_{\mathrm{r}} + \mathrm{i}\mathcal{D}_{\mathrm{i}}\,, \tag{3.21a}$$

$$\mathcal{D}_r + i\mathcal{D}_i = \Big[\cos(2\alpha_{ij} - 2\gamma_{ij}) + i\sin(2\alpha_{ij} - 2\gamma_{ij})\Big]_{\mathcal{D}} f(\beta_{ij}, \ell_{\min}, \ell_{\max})\,, \tag{3.21b}$$

where the radial functions are given by,

$$_{\mathcal{D}/\mathcal{I}}f(\beta, \ell_{\min}, \ell_{\max}) = \sum_{\ell=\ell_{\min}}^{\ell_{\max}} \sqrt{\frac{2\ell+1}{4\pi}}\, {}_{\mathcal{D}/\mathcal{I}}f_{\ell}(\beta)\,, \tag{3.22}$$

where the functions ${}_{\pm 2}f_{\ell}(\beta)$ are expressed in terms of P_{ℓ}^2 Legendre polynomials and are given by the following explicit mathematical forms,

$$\begin{aligned} {}_{\mathcal{D}/\mathcal{I}}f_{\ell}(\beta) = 2\frac{(\ell-2)!}{(\ell+2)!}\sqrt{\frac{2\ell+1}{4\pi}}\Bigg[&- P_{\ell}^2(\cos\beta)\left(\frac{\ell-4}{\sin^2\beta} + \frac{1}{2}\ell(\ell-1) \pm \frac{2(\ell-1)\cos\beta}{\sin^2\beta}\right) \\ &+ P_{\ell-1}^2(\cos\beta)\left((\ell+2)\frac{\cos\beta}{\sin^2\beta} \pm \frac{2(\ell+2)}{\sin^2\beta}\right)\Bigg]\,. \end{aligned} \tag{3.23}$$

Finally the Stokes parameters corresponding to the respective scalar fields can be computed by evaluating the following expressions,

$$\begin{aligned} \begin{bmatrix} Q_i \\ U_i \end{bmatrix}_{E/B} = \sum_{j=1}^{N_{\mathrm{pix}}} \Bigg\{ &{}_{\mathcal{I}}f(\beta_{ij}, \ell_{\min}, \ell_{\max}) \begin{bmatrix} \cos(2\alpha_{ij} + 2\gamma_{ij}) & \sin(2\alpha_{ij} + 2\gamma_{ij}) \\ -\sin(2\alpha_{ij} + 2\gamma_{ij}) & \cos(2\alpha_{ij} + 2\gamma_{ij}) \end{bmatrix} \begin{bmatrix} Q_j \\ U_j \end{bmatrix} \\ &\pm {}_{\mathcal{D}}f(\beta_{ij}, \ell_{\min}, \ell_{\max}) \begin{bmatrix} \cos(2\alpha_{ij} - 2\gamma_{ij}) & \sin(2\alpha_{ij} - 2\gamma_{ij}) \\ \sin(2\alpha_{ij} - 2\gamma_{ij}) & -\cos(2\alpha_{ij} - 2\gamma_{ij}) \end{bmatrix} \begin{bmatrix} Q_j \\ U_j \end{bmatrix} \Bigg\} 0.5\Delta\Omega\,, \end{aligned} \tag{3.24}$$

where all the symbols have their usual meaning. The above expression can be cast in the further simplified form,

$$\begin{aligned} {}_{+2}X_{E/B} &= 0.5\Delta\Omega \sum_{j=1}^{N_{\mathrm{pix}}} {}_{\mathcal{I}}f(\beta_{ij}) e^{-i2(\alpha_{ij}+\gamma_{ij})}\, {}_{+2}X_j \pm {}_{\mathcal{D}}f(\beta_{ij}) e^{i2(\alpha_{ij}-\gamma_{ij})}\, {}_{+2}X_j^*\,, & \text{(3.25a)} \\ &= 0.5\Big\{\mathcal{I}^* \circ {}_{+2}X \pm \mathcal{D} \circ {}_{+2}X^*\Big\}\,, & \text{(3.25b)} \end{aligned}$$

where in Eq. (3.25a) we have suppressed the explicit multipole dependence of functions ${}_{\pm 2}f$ for brevity and in Eq. (3.25b) $\circ$ denotes a convolution. $\Rightarrow$ Here it will be nice to interpret $e^{i2\gamma}[E - iB]$. We don't understand this as of now.

$\Rightarrow$ Recheck the math described below The function $\mathcal{I}$ is a band limited version of the delta function ($\lim_{\ell\to\infty}\mathcal{I} = \delta(\hat{n}_i - \hat{n}_j)$). When interpreted as a matrix it is a band limited version of the identity matrix. Though it has non vanishing off diagonal elements ($\mathcal{I} \neq 0$ when $\hat{n}_i \neq \hat{n}_j$) owing to the band limit, for all practical purposes $\mathcal{I}$ acts like an identity operator as is confirmed by the following set of identities: (i) $\mathcal{I} * \mathcal{I} = \mathcal{I}$; (ii) $\mathcal{D} * \mathcal{I} = \mathcal{D}$. Also $\mathcal{D}^*$ is the inverse of $\mathcal{D}$ in this band limited sense: $\mathcal{D}^* * \mathcal{D} = \mathcal{I}$. It is useful to note that the

operator $\mathcal{D}$ is a complex but symmetric matrix and $\mathcal{I}$ is an Hermitian operator. Using these properties of the operators $\mathcal{I}$ and $\mathcal{D}$, one can verify that the real space operators satisfy the following identities,

$$\bar{O}_E * \bar{O}_E = \bar{O}_E \;\; ; \;\; \bar{O}_B * \bar{O}_B = \bar{O}_B \,, \tag{3.26a}$$

$$\bar{O}_E * \bar{O}_B = 0 \,, \tag{3.26b}$$

$$\bar{O}_E + \bar{O}_B = \mathcal{I} \,, \tag{3.26c}$$

which are the real space analogues of Eq. (2.14). While testing the above stated identities one encounters terms like $\mathcal{D} * \mathcal{I}^*, \mathcal{I}^* * \mathcal{I}$ and $\mathcal{I} * \mathcal{I}^*$ which cannot be simply interpreted, but they always occur in pairs with opposite signs, hence exactly canceling each other.

Note that unlike in the harmonic case, the sum of the operators is not exactly an identity matrix. This non-exactness is representative of the loss of information resulting from making this transformation on the measured data with some imposed band limit. Forcing the sum of the operators to be exactly an identity matrix compromises the orthogonality property of the $\bar{O}_E$ & $\bar{O}_B$ operators, which is exact.

3.4 Visualizing the convolution kernels

Evaluating the local kernels: Let us consider the case when one of the coordinates coincides with the north pole $\hat{z} = (0, 0)$ (this refers to the point $\theta_0 \to 0$ while moving along the longitude $\phi_0 = 0$). In this case the Euler angles in the $z - y1 - z2$ convention are simply given by: $(\alpha, \beta, \gamma) = (\phi_i, \theta_i, 0)$, where (θ_i, ϕ_i) denote the coordinates of the location $\hat{n}_i$. Since the Euler angle $\gamma = 0$ when rotations are defined with respect to the pole, the respective kernels simplify to the following forms,

$$\mathcal{M}(\hat{z}, \hat{n}_i) = \sum_\ell {}_0a_{\ell 2}\, {}_0Y_{\ell 2}(\hat{n}_i) \,; \tag{3.27a}$$

$$\mathcal{I}(\hat{z}, \hat{n}_i) = \sum_\ell {}_{-2}a_{\ell 2}\, {}_{-2}Y_{\ell 2}(\hat{n}_i) \;\; ; \;\; \mathcal{D}(\hat{z}, \hat{n}_i) = \sum_\ell {}_2a_{\ell 2}\, {}_2Y_{\ell 2}(\hat{n}_i) \,, \tag{3.27b}$$

where ${}_sa_{\ell 2} = \sqrt{\frac{2\ell+1}{4\pi}} \;\; \forall \;\; s \in [0, -2, +2]$. The convolution kernels centered around any other location $\hat{n}_j = (\theta_j, \phi_j)$ are simply given by evaluating the respective spherical harmonic sums: $\sum_{\ell m} {}_sa_{\ell m}\, {}_sY_{\ell m}(\hat{n}_i)$ using the rotated harmonic coefficients given by: ${}_sa_{\ell m} = D^\ell_{m2}(\phi_j, \theta_j, 0)\, {}_sa_{\ell 2}$, where D^ℓ_{2m} are the Wigner-D functions. These rotation operations can be carried out using inbuilt Healpix routine *rotate_alm*, while the convolution kernels can be synthesized by evaluating the respective spherical harmonic sums using the *alm2map* routine. ⇒ Make parallels with instrument beam analysis here ? Or is it trivial since its obvious that all convolution problems can be cast in this form.

We compute the local convolution kernels using the procedure described above. To given an intuition for how these kernels vary as a function of position of the central pixel we depict in Fig. 3 the kernels at a few different locations. For illustration these functions are sampled at a very high Healpix resolution parameter of NSIDE=2048. All the plots have been rotated such that the central location $\hat{n}_j$ marked by the black circle are in the centre of the figure. The horizontal and vertical lines that pass through the central black circle mark the local latitude and longitude respectively.

The real and imaginary part of the kernel $\mathcal{M}$ are identical irrespective of changes in the galactic latitude and longitude of the central pixel. Note that these functions are not

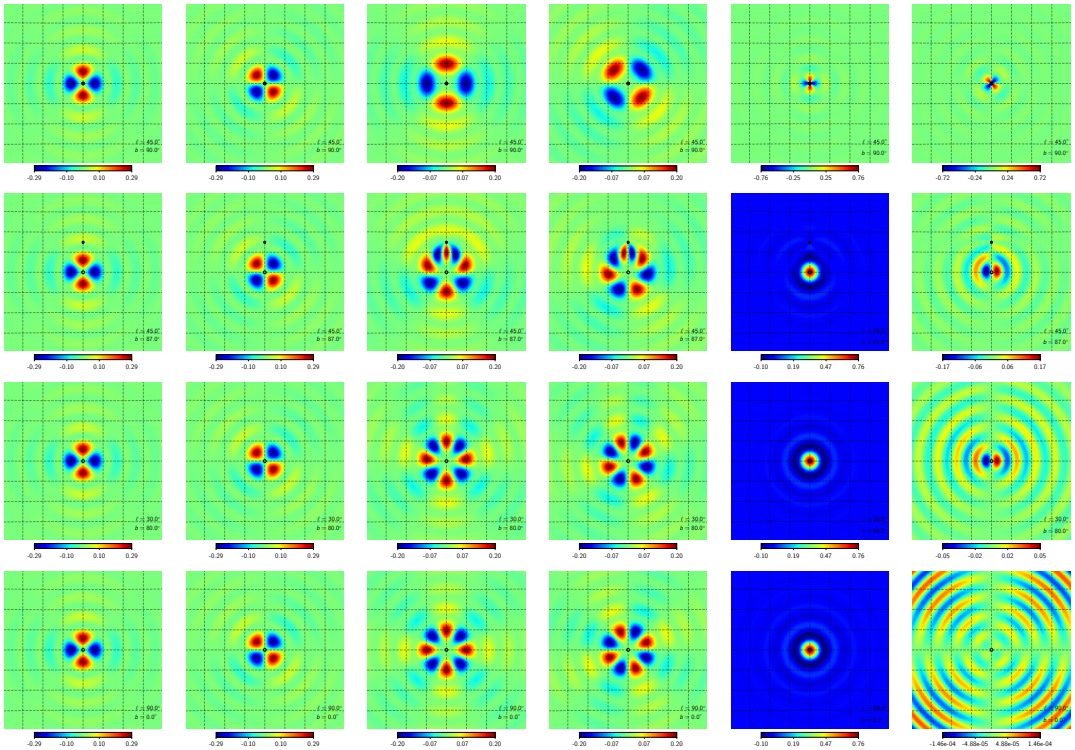

(xix) $\mathcal{M}_r$ (xx) $\mathcal{M}_i$ (xxi) $\mathcal{D}_r$ (xxii) $\mathcal{D}_i$ (xxiii) $\mathcal{I}_r$ (xxiv) $\mathcal{I}_i$

Figure 3. This panel of figure depicts the various parts of the convolution kernel, discussed in Sec. 3. These kernels have been evaluated with the band limit: $\ell \in [2, 192]$ but sampled at the Healpix resolution parameter NSIDE=2048 for visual appeal. The size of each panel is approximately $16^\circ \times 16^\circ$ and the grid lines are marked at 2 degree separations. The black circles denotes the position of the central pixel around which the convolution kernels have been evaluated while the black star marks the location of the north galactic pole. The four rows depict the kernels at different location on the sphere and the galactic coordinates of the central pixel are specified in each panel.

distorted when a part of the domain overlaps with the poles, as can be seen in the first three rows of Fig. 3. Both these facts can be associated with the fact that this function does not depend on the Euler angle γ. From Eq. (3.7) and Eq. (3.14) it is clear that $\mathcal{M}_r$ and $\mathcal{M}_i$ can be interpreted in the following ways,

$$\begin{bmatrix} E = -\mathcal{M}_r \\ B = +\mathcal{M}_i \end{bmatrix} \leftarrow \begin{bmatrix} Q = \delta(\hat{n} - \hat{n}_j) \\ U = 0 \end{bmatrix} \quad ; \quad \begin{bmatrix} E = -\mathcal{M}_i \\ B = -\mathcal{M}_r \end{bmatrix} \leftarrow \begin{bmatrix} Q = 0 \\ U = \delta(\hat{n} - \hat{n}_j) \end{bmatrix}, \tag{3.28a}$$

$$\begin{bmatrix} Q = -\mathcal{M}_r \\ U = -\mathcal{M}_i \end{bmatrix} \leftarrow \begin{bmatrix} E = \delta(\hat{n} - \hat{n}_j) \\ B = 0 \end{bmatrix} \quad ; \quad \begin{bmatrix} Q = +\mathcal{M}_i \\ U = -\mathcal{M}_r \end{bmatrix} \leftarrow \begin{bmatrix} E = 0 \\ B = \delta(\hat{n} - \hat{n}_j) \end{bmatrix}. \tag{3.28b}$$

The kernels $\mathcal{D}$ & $\mathcal{I}$ vary significantly as a function of galactic latitude of the central pixel as seen in the last four columns of Fig. 3. These kernels show a two fold symmetry in the vicinity of the poles and this arises due to Euler angle $\gamma \approx 0$ here and therefore $e^{i2(\alpha \pm \gamma)} \approx e^{i2\alpha}$. Note that in this region, the azimuthal profile of the real and imaginary part of these kernels is similar to $\mathcal{M}_r$ and $\mathcal{M}_i$ respectively. This also explains why the imaginary part of the band limited delta function $\mathcal{I}$ contributes just as much as the real part in these regions. On moving to lower latitudes, $\mathcal{D}$ quickly transitions to having a four fold symmetry while $\mathcal{I}$ transitions

to being dominated by the real part and behaves more like the conventional delta function. This transition can be most easily understood in the flat sky limit where $\gamma = -\alpha$ which leads to the resultant 4 fold symmetry seen for $\mathcal{D}$ owing to $e^{i2(\alpha-\gamma)} = e^{i4\alpha}$ and $\mathcal{I}$ being dominated by the real part owing to $e^{-i2(\alpha+\gamma)} = 1 + i0$. Since the flat sky approximation has most validity in the proximity of the equator these limiting tendencies of the respective kernels are seen in the bottom row of Fig. 3 which depict the kernels evaluated at the equator $b = 0°$. The middle two row depict the kernels evaluated at a latitudes of $b = 87°$ & $80°$ and serve to indicate the rate of this transition. These kernels are invariant under changes in longitude of the central pixel, the latitude being held fixed, as one may have expected.

3.5 Quantifying the non-locality of E & B modes

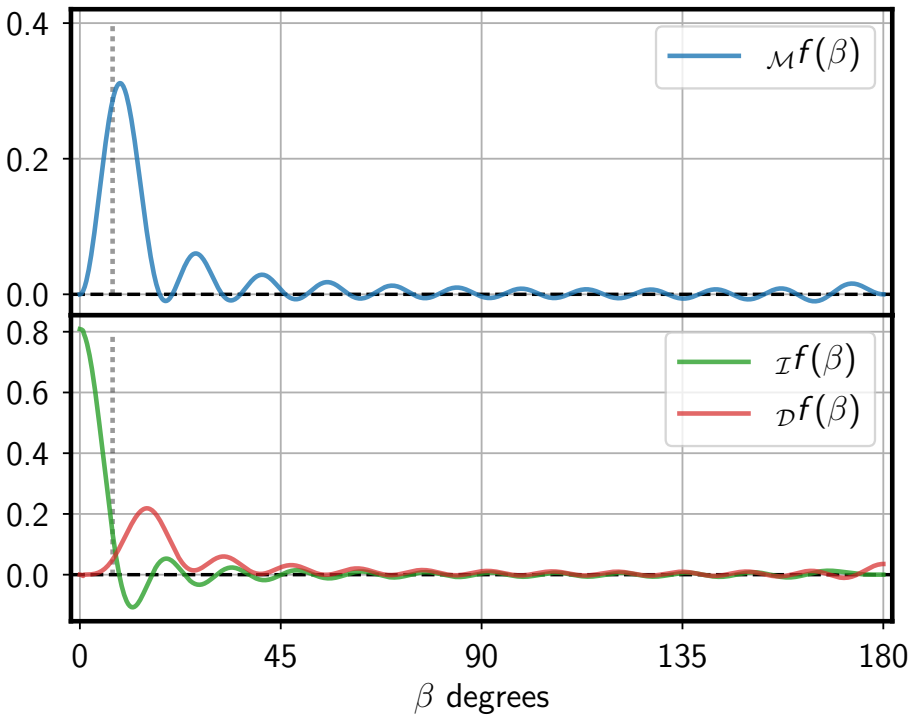

Figure 4. The figure depicts the radial part of the convolution kernels. These radial function have been evaluated with the band limit fixed at $\ell \in [2, 24]$. The vertical dashed line marks the approximate Healpix pixel size of a NSIDE=8, which is the lowest resolution that allows access to $\ell_{\rm max} = 24$.

Fig. 3.4 and the surrounding discussion provides a quantative understanding of the azimuthal dependence of various kernels, however it is difficult to assess the radial nature of these kernels from these figures. The radial part determines the non-locality of the respective operators and encodes all the multipole dependence. We compute the radial kernels $_{\mathcal{M}}f, _{\mathcal{D}}f$ & $_{\mathcal{I}}f$ by evaluating the respective multipole sums in Eq. (3.5b) and Eq. (3.22) in the band limit $\ell \in [2, 192]$ and the resultant functions are depicted in Fig. 4.

Recall that $_{\mathcal{M}}f$ is the radial part of the kernel that translates the Stokes parameters Q & U to scalars E & B and vice versa. Note that $_{\mathcal{M}}f$ has a vanishing contribution from the location of the central pixel ($\beta \to 0$) as seen in Fig. 4 and one can show that that $_{\mathcal{M}}f(\beta = \pi) = 0$. The coordinate dependence of the Stokes parameters cannot be integrated

out in the vicinity of the locations $\beta = 0, \pi$ due to the fact that the azimuthal angles become ill defined here therefore this nature of ${}_{\mathcal{M}}f$ is necessary to ensure that the derived fields behave as scalars. Similarly while deriving the Stoke field from the scalars E & B this nature of ${}_{\mathcal{M}}f$ is necessary to ensure that the necessary coordinate dependencies are integrated in. ${}_{\mathcal{D}}f$ shows a similar behaviour, it has a vanishing contribution in the vicinity of the central pixel and dominantly contributes in regions which are approximately at least 1 pixel distance away from the central pixel as seen in Fig. 4. ${}_{\mathcal{I}}f$ is the radial part of the band limited delta function $\mathcal{I}$ and expectedly contributes the most at the location of the central pixel.

The band limit dependence: It is clear from previous discussions that the scalar field E & B constructed at a location depends on the Stokes field in the surrounding regions. We further quantify this non-locality by studying the radial extent of the kernels and its dependence on the maximum multipole accessible for analysis. To carry out this study we evaluate the radial functions for different values of $\ell_{\rm max}$, while keeping the lowest multipole fixed at $\ell_{\rm min} = 2$. The resultant set of radial function are depicted in Fig. 5, where all the function have been normalized such that their global maxima is set to unity. We note that on increasing $\ell_{\rm max}$ the radial kernels shift left, attaining their global maxima at progressively small angular distance from the central pixel. The amplitude of these radial function scales up as $\propto \ell^2_{\rm max}$. At intermediate values of β, the envelope of the radial functions is fit well by a power law $\propto \beta^{-n}$, the details of this fit can be seen in Fig. 5. We observe that the radial functions computed by evaluating the multipole sums to different maximum multipoles are self similar and follow an interesting telescoping and scaling property,

$$ {}_{r}f(\beta, 2, \ell_{\rm max}) \approx \left[\frac{\ell_{\rm max}}{\ell'_{\rm max}}\right]^2 {}_{r}f(\beta' = \frac{\ell_{\rm max}}{\ell'_{\rm max}}\beta, 2, \ell'_{\rm max}) \,, $$

where ${}_{r}f$ denotes all the different radial functions.

It is useful to define a characteristic radius of the region from which the scalar fields evaluated at a point get most of their contribution from. Since the primarily interest is in the non-locality of the scalar modes E & B we define the abscissa at which the function ${}_{\mathcal{M}}f(\beta, \ell_{\rm min} = 2, \ell_{\rm max})$ transits to being monotonously below 1% of the maxima of the function as the non-locality parameter: β_o. For $\ell_{\rm max} = 24$, the maximum multipole accessible on a Nside=8 Healpix map, the non-locality parameter $\beta_0 = 180^\circ$ as the radial function never falls monotonously below 1% of its global maxima. Using this fact and the self similar property of the radial functions, we define the following empirical relation: $\beta_o = \min(180, 180\frac{24}{\ell_{\rm max}})$, as a means of estimating the non-locality parameter given the maximum multipole $\ell_{\rm max}$ accessible for analysis.

4 Generalized operators

The azimuthal of the convolution kernel $\mathcal{M}$ could have been been argued to have the form $e^{-i2\alpha}$ by requiring to construct a spin-0 field given some spin-2 fields. In this sense there is no freedom in the choice of the azimuthal dependence of the convolution kernels. The radial part of this kernel however is determined by the basis functions. It is possible to generalize these convolution kernels by choosing alternate forms for the radial functions, without affecting the parity properties of the scalar fields E & B.

We can characterize different forms of the radial kernel by introducing the following harmonic space operator,

$$ \tilde{\mathcal{G}} = \begin{bmatrix} g^E_\ell & 0 \\ 0 & g^B_\ell \end{bmatrix} , \tag{4.1} $$

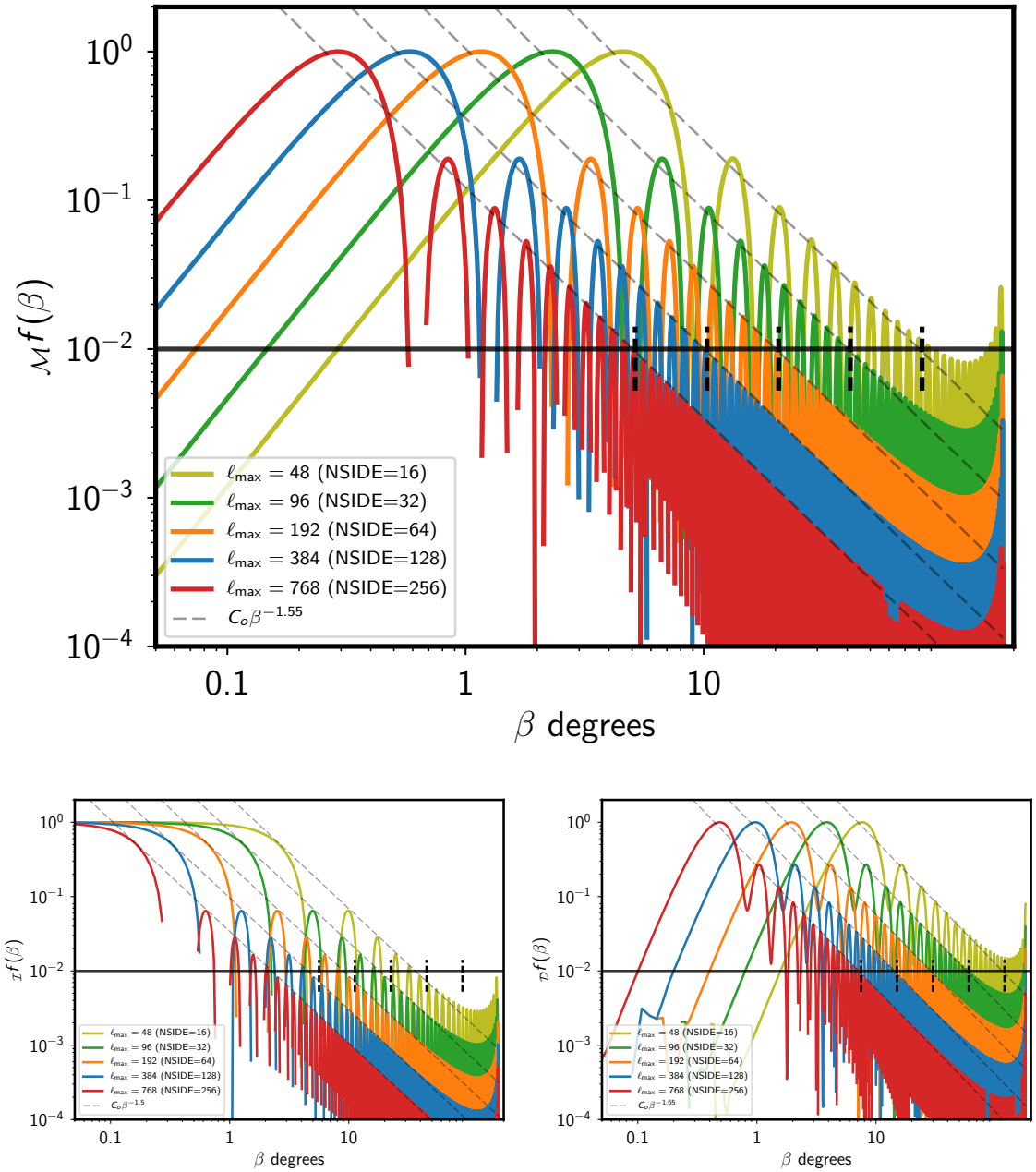

Figure 5. The top panel depicts the radial function $_{\mathcal{M}}f(\beta, \ell_{\rm min}, \ell_{\rm max})$ while the bottom left and right panels show the radial functions $_{\mathcal{I}}f(\beta, \ell_{\rm min}, \ell_{\rm max})$ & $_{\mathcal{D}}f(\beta, \ell_{\rm min}, \ell_{\rm max})$ respectively, for fixed $\ell_{\rm min} = 2$ and different $\ell_{\rm max}$ as indicated by their legends. All the curves have been normalized such that the maximum of the curve is set to unity. The horizontal solid black line marks the location where the amplitude of the kernel falls below 1% of its maximum. The slanted dashed black lines indicate a power law fit (by eye) to the envelope of the radial functions. While the envelopes for function $_{\mathcal{M}}f(\beta)$ & $_{\mathcal{I}}f(\beta)$ are fit well by the power law $\propto \beta^{-1.5}$, the envelope for the function $_{\mathcal{D}}f(\beta)$ is seen to have a slightly steeper slope $\propto \beta^{-1.65}$.

where the functions g_ℓ^E and g_ℓ^B represent the harmonic representation of the modified radial functions and can in the most general case be chosen to be different for E and B modes. To

simplify the discussion and without loosing generality we proceed by setting $g_\ell^E = g_\ell^B = g_\ell$. Once we have made a choice for these harmonic functions, we can define the real space operator $\bar{O}'$ which translates Stokes Q & U to scalars E & B and the inverse operator $\bar{O}'^{-1}$ in the following manner,

$$\bar{O}' = {}_0\mathcal{Y} * \tilde{T}^{-1} * \tilde{\mathcal{G}} * {}_2\mathcal{Y}^\dagger * \bar{T}\,, \tag{4.2a}$$

$$\bar{O}'^{-1} = \bar{T}^{-1} * {}_2\mathcal{Y} * \tilde{\mathcal{G}}^{-1} * \tilde{T} * {}_0\mathcal{Y}^\dagger \tag{4.2b}$$

where we have used the primed notation to distinguish these generalized operators from the default operators defined in Sec. 3.1 and Sec. 3.2. Note that for an arbitrary choice of $\tilde{\mathcal{G}}$ only one of the operators in Eq. (4.2) is well defined, since $\tilde{\mathcal{G}}^{-1}$ may be ill defined. If we require both the forward and inverse operators to be well defined, then we are constrained in choosing $\tilde{\mathcal{G}}$ such that it has a valid inverse. As we will see this will be an important criteria to recover the standard CMB spectra. The radial part of these generalized convolution kernels is given by the following expressions,

$$G_{QU\to EB}(\beta) = G(\beta) = \sum_{\ell=2}^{\ell_{\rm max}} g_\ell \frac{2\ell+1}{4\pi}\sqrt{\frac{(\ell-2)!}{(\ell+2)!}}P_\ell^2(\cos\beta) \tag{4.3a}$$

$$G_{EB\to QU}(\beta) = G^{-1}(\beta) = \sum_{\ell=2}^{\ell_{\rm max}} g_\ell^{-1} \frac{2\ell+1}{4\pi}\sqrt{\frac{(\ell-2)!}{(\ell+2)!}}P_\ell^2(\cos\beta)\,, \tag{4.3b}$$

where g_ℓ are the same multipole function as those appearing in $\tilde{\mathcal{G}}$. Given this general definition for the radial function $G(\beta)$, note that the default radial function ${}_{\mathcal{M}}f$ is just a special case resulting from the choice $\tilde{\mathcal{G}} = \mathbb{1}$ ($g_\ell = 1$). Note that for this choice of $\tilde{\mathcal{G}}$ the inverse is trivial $\tilde{\mathcal{G}}^{-1} = \tilde{\mathcal{G}}$ and therefore $G^{-1}(\beta) = G(\beta)$.

While defining these generalized operators, it seems more natural to choose the real space function $G(\beta)$ as compared to choosing the multipole function g_ℓ. Using the orthogonality property of associated Legendre polynomials it can be shown that the harmonic function g_ℓ is given by the following integral over the radial function $G(\beta)$,

$$g_\ell = 2\pi\sqrt{\frac{(\ell-2)!}{(\ell+2)!}}\int_0^\pi G(\beta)P_\ell^2(\cos\beta)d\cos\beta\,. \tag{4.4}$$

To ensure that the resultant field is a spin-0 field, it is important to note that the radial function $G(\beta)$ has to be necessarily chosen such that it vanishes at $\beta = 0$ and $\beta = \pi$.

An arbirtrary $G(\beta)$ for which $g_\ell \neq 1$ can be equivalently thought in terms of the standard E and B mode fields being convolved with some circularly symmetric instrument beam. Note that in contrast to the radial function $G(\beta)$ an instrumental beam function appropriately normalized has the property $B(\beta) \to 1$ as $\beta \to 0$. We clarify that the $B(\beta)$ refers to the effective beam acting to smooth the scalar E & B mode maps. A circularly symmetric beam $B(\beta)$ defined at the pole can be expressed in the Legendre polynomial P_ℓ^0 basis as follows,

$$B(\beta) = \sum_{\ell=0}^{\ell_{\rm max}} \frac{2\ell+1}{4\pi} b_\ell P_\ell^0(\cos\beta)\,, \tag{4.5}$$

where b_ℓ denote the coefficients of expansion. $\Rightarrow$ Note that one can directly get E and B mode maps resulting from convolution with a non-circular beam by chosing the function g_ℓ to have some m dependence.

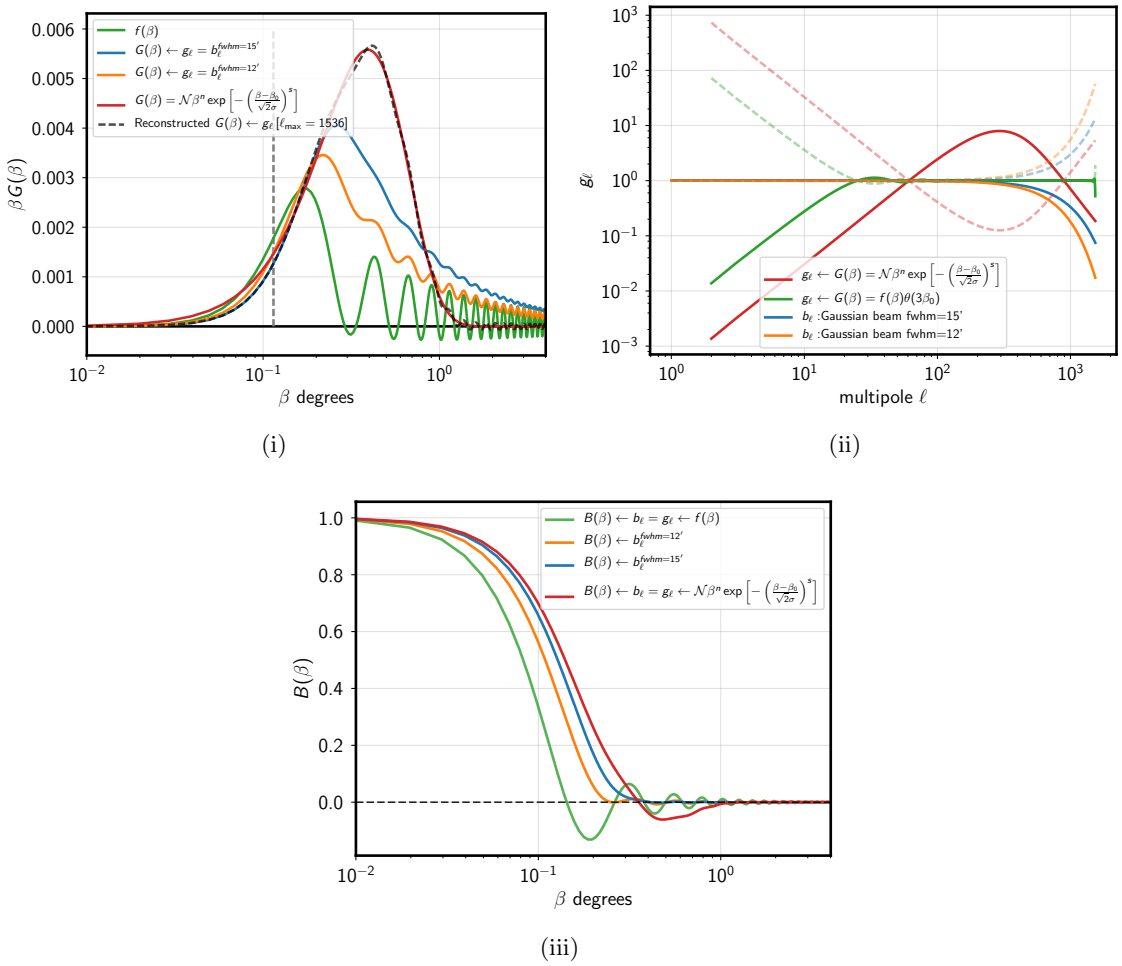

Figure 6. *Left:* The vertical dashed gray line depicts the approximate pixel size $\Delta_{\rm pix} = \sqrt{\frac{4\pi}{N_{\rm pix}}}$ of a Nside=512 Healpix map. The green line depicts the default radial kernel $f(\beta)$ defined in Eq. (3.5). The blue and orange lines depict the modified radial function resulting the beam harmonics b_ℓ corresponding to Gaussian beams with fwhm=15 & 12 arcminutes respectively. The red curve depicts an example modified radial function: $G(\beta) = \mathcal{N}\beta^n \exp\left[-\left(\frac{\beta-\beta 0}{\sqrt{2}\sigma}\right)^s\right]$ with parameters set to the following values $[n = 1;\, \beta_0 = 0;\, \sigma = 2\Delta_{\rm pix};\, s = 1.5]$. The black dashed curve depicts the band limited reconstruction of the modified radial function $G(\beta)$. We intentionally have plotted $\beta G(\beta)$ to clearly depict the high β behavior of these functions. *Middle:* This figure depicts the harmonic representation of the respective radial functions as indicated by the legend. The dashed curves of the corresponding color depict the inverse of the harmonic functions. *Right:* This figure depicts the beam function $B(\beta)$ evaluated from interpreting the respective harmonic functions as those corresponding to an instrument beam.

Though the real space behavior of these two function $G(\beta)$ and $B(\beta)$ has important differences, in harmonic space they play identical roles. Therefore it is possible to interpret the beam harmonic coefficients as those representing some modified radial kernel. Fig. 6(ii) depicts the harmonic functions $g_\ell(b_\ell)$ for the respective radial kernel and beams. The modified radial kernel resulting from Gaussian beams with fwhm $= 15' \,\&\, 12'$ are depicted in Fig. 6(i) as blue and orange curves respectively. Note that instruments beams tend to increase the

non-locality parameter β_0, indicated by the shifting right of the maxima of the respective kernels, as one may have expected. The red curve depicts a modified radial kernel which by construction has a very small β_0. Similarly it is possible to interpret the harmonic representation g_ℓ of the radial function $G(\beta)$ as those corresponding to some instrument beam function. The beam function corresponding to the default radial kernel ($g_\ell = 1$) is merely a band limited representation of the delta function depicted by the green curve Fig. 6(iii), while the red curve depicts the same for the modified radial kernel.

4.1 Recovering the default E and B mode spectra

The generalized convolution kernels defined in the previous section, when operated on the Stokes vector returns some scalar E' and B' mode maps,

$$\bar{S}' = \bar{O}' * \bar{P} \tag{4.6}$$

which as we show are mere filtered version of he standard E and B modes maps. The harmonic representation g_ℓ of the radial function $G(\beta)$ can be simply interpreted as the harmonic coefficients of some azimuthally symmetric beam $B(\beta) = \sum_\ell \frac{2\ell+1}{4\pi} g_\ell P_\ell^0(\cos\beta)$. The spectra of the scalar fields E' and B' derived using the real space operators constructed using an arbitrary radial function $G(\beta)$ are related to the spectra of the standard E and B fields via the following relation,

$$C_\ell^{EE,BB,EB} = C_\ell^{E'E',B'B',E'B'}/g_\ell^2\,, \tag{4.7a}$$

$$C_\ell^{TE,TB} = C_\ell^{TE',TB'}/g_\ell\,, \tag{4.7b}$$

where C_ℓ denotes the angular power spectra and T refers to the temperature anisotropy map. Therefore the standard E and B mode spectra can be recovered from the modified fields E' and B' and their accurate recovery only relies on the inverse of the harmonic functions $1/g_\ell$ being well behaved, which can be ensured by making a suitable choice for the radial function $G(\beta)$. Examples of various forms of $G(\beta)$, its harmonic representation g_ℓ (and its inverse $1/g_\ell$) and the corresponding beam $B(\beta)$ are depicted in Fig. 6.

5 Discussion

A similar equation for real space E & B operators was derived in [1], however those results were derived for the flat sky case and did not explicitly derive the radial kernel. ⇒ A discussion on this should be in the conclusions.

In this article we have cast the standard CMB polarization analysis operations in a vector matrix notation. Using this concise notation we derive the real space operators that translate the Stokes vector $\bar{P}$ to the vector of scalars $\bar{S}$ and vice versa. We explicitly demonstrated that this real space operation can be simply interpreted as a convolution over the complex field $[Q-iU]$ (or $[E+iB]$) with an effective complex beam which is fully expressed in terms of the $Y_{\ell 2}$ spherical harmonic functions. We also use this vector matrix notation to derive real space operators which allow the direct decomposition of the full Stokes vector $\bar{P}$ into the vector $\bar{P}_E$ and $\bar{P}_B$ that correspond to the respective scalar modes.

Given the effective beam interpretation of these real space operators we derive the harmonic coefficients of these effective beams at the north galactic pole. Using these harmonic coefficients we provide a prescription for computing the convolution kernels at any position on the sphere using the standard Healpix built in functions. The procedure is equivalent

to parallel transporting the beam at the north pole to any desired location on the sphere. We implement the prescription to compute the kernel at different location on the sphere and provide simple explanations in terms of Euler angles for the observed variations.

These real space convolution kernels provide a spatially intuitive way of understanding the construction of the scalar modes. We explicitly show that the kernels separates into an band limit independent azimuthal operation around any given direction which is primarily responsible for requisite decomposition, while the band limit dependent radial weights can be interpreted as some isotropic smoothing operation. These radial weights primarily determine the non-local dependence of the construction of the respective fields at any location on the Stoke field. We define the parameter β_0 as a means to characterize the non-locality and show that β_0 scales $\propto \ell_{\rm max}^{-1}$. We show that this non-locality parameter also characterized the non-locality of the $\bar{O}_{E/B}$ operators.

Finally we present the generalized real space operators $\bar{O}'$, which are derived by allowing the radial function to vary from its default form. We derive constraints on the modifications to these radial function by demanding the inverse operator to be well defined. We argue that these modifications to the radial kernel can be be interpreted as a some smoothing smoothing operation on the scalar fields with a circularly symmetric instrument beam. We also show that as long as these radial function are invertible, the standard spectra can always be recovered from these modified E' & B' maps. The main advantage of modifying these radial function is the ability to generate more locally defined E and B mode maps. This could potentially be useful in reducing foreground contamination on large angular scales in a full sky E/B analysis. Also defining more locally constructed scalar fields E & B can be used to circumvent the power leakage nuisance. We explore and demonstrate the working of these ideas in the next paper in this series.

6 Appendix

6.1 Product of spin spherical harmonics

The spin spherical harmonics are related to the Wigner D functions via the following relations,

$$D^{\ell}_{-sm}(\alpha,\beta,\gamma) = \sqrt{\frac{4\pi}{2\ell+1}}\, {}_sY_{\ell m}(\beta,\alpha)e^{-is\gamma}\,, \tag{6.1}$$

where α, β & γ can be thought of as Euler angles for some rotation.

The product of two different spherical harmonic functions can be expressed in terms of the Wigner D functions and simplified using their identities. In particular we are interested in products of spherical harmonic function of the following kind,

$$\begin{aligned}
\sum_m {}_{s_1}Y_{\ell m}(\theta_e,\phi_e)\,{}_{s_2}Y^*_{\ell m}(\theta_q,\phi_q) &= \frac{2\ell+1}{4\pi}\sum_m D^{\ell}_{-s_1 m}(\phi_e,\theta_e,0)D^{*\ell}_{-s_2 m}(\phi_q,\theta_q,0)\,, && \text{(6.2a)}\\
&= \frac{2\ell+1}{4\pi}\sum_m D^{\ell}_{-s_1 m}(\phi_e,\theta_e,0)D^{\ell}_{m-s_2}(0,-\theta_q,-\phi_q)\,, && \text{(6.2b)}\\
&= \frac{2\ell+1}{4\pi}D^{\ell}_{-s_1-s_2}(\alpha_{qe},\beta_{qe},\gamma_{qe})\,, && \text{(6.2c)}\\
&= \sqrt{\frac{2\ell+1}{4\pi}}\,{}_{s_1}Y_{\ell-s_2}(\beta_{qe},\alpha_{qe})e^{-is_1\gamma_{qe}} && \text{(6.2d)}
\end{aligned}$$

where we have used some standard identities of the Wigner D functions to transition between then equations [4]. Note that the Euler angles $(\alpha, \beta, \gamma) = (0, -\theta_q, -\phi_q)$ correspond to a rotation that aligns the local cartesian coordinate at $\hat{n}_q$ with that at the pole and the Euler angles $(\alpha, \beta, \gamma) = (\phi_e, \theta_e, 0)$ correspond to rotations that align the local cartesian coordinates at the pole with those at the location $\hat{n}_e$. Hence the net rotation operation is that of aligning the local cartesian coordinates at location $\hat{n}_q$ with those at location $\hat{n}_e$ and therefore the final results are expressed in terms of Euler angles: $(\alpha_{qe}, \beta_{qe}, \gamma_{qe})$.

Since the following equation holds true,

$$\sum_m {}_{s_1}Y_{\ell m}(\theta_e, \phi_e)\,{}_{s_2}Y^*_{\ell m}(\theta_q, \phi_q) = \sum_m {}_{-s_1}Y^*_{\ell m}(\theta_e, \phi_e)\,{}_{-s_2}Y_{\ell m}(\theta_q, \phi_q)\,, \tag{6.3}$$

this sum over product of spin spherical harmonic functions can be equally expressed in terms of the Euler angles corresponding to the inverse rotations. Using the same algebra as given above, it is possible to show that

6.2 Relation between the real space operators and the spin raising/lowering operators

References

[1] M. Zaldarriaga, *The nature of the E-B decomposition of CMB polarization*, *Phys. Rev. D* **64** (jun, 2001) 103001, [0106174].

[2] M. Zaldarriaga and U. Seljak, *All-sky analysis of polarization in the microwave background*, *Phys. Rev. D* **55** (feb, 1997) 1830–1840, [astro-ph/9609170].

[3] J. N. Goldberg, A. J. Macfarlane, E. T. Newman, F. Rohrlich and E. C. G. Sudarshan, *Spin-s Spherical Harmonics and* ð, *J. Math. Phys.* **8** (nov, 1967) 2155–2161.

[4] D. A. Varshalovich, A. N. Moskalev and V. K. Khersonskii, *Quantum Theory of Angular Momentum (World Scientific)*. World Scientific, 1988.